A Nucleic Acid Base Analog FRET-pair Facilitating Detailed Structural Measurements in Nucleic Acid Containing Systems

Karl Börjesson,[†] Søren Preus,[‡] Afaf H. El-Sagheer,[§,#] Tom Brown,[§] Bo Albinsson,[†] and L. Marcus Wilhelmsson[*,†]

[†]Department of Chemical and Biological Engineering/Physical Chemistry, Chalmers University of Technology, S-41296 Gothenburg, Sweden, [‡]Department of Chemistry, University of Copenhagen, Universitetsparken 5, DK-2100 Copenhagen, Denmark, [§]School of Chemistry, University of Southampton, Highfield, Southampton, SO17 1BJ, UK, [#]Chemistry Branch, Department of Science and Mathematics, Faculty of Petroleum and Mining Engineering, Suez Canal University, Suez, Egypt.

E-MAIL ADDRESS: marcus.wilhelmsson@chalmers.se

RECEIVED DATE (to be automatically inserted after your manuscript is accepted if required according to the journal that you are submitting your paper to)

CORRESPONDING AUTHOR FOOTNOTE: L. Marcus Wilhelmsson: telephone number: +46 31 7723051 and fax number: +46 31 7723858.

Abstract

We present the first nucleobase analog fluorescence resonance energy transfer (FRET)-pair. The pair consists of tC^O, 1,3-diaza-2-oxophenoxazine, as an energy donor and the newly developed tC_{nitro}, 7-nitro-1,3-diaza-2-oxophenothiazine, as an energy acceptor. The FRET-pair successfully monitors distances covering up to more than one turn of the DNA duplex. Importantly, we show that the rigid stacking of the two base analogs, and consequently excellent control of their exact positions and orientations, results in a high control of the orientation factor and hence very distinct FRET changes as the number of bases separating tC^O and tC_{nitro} is varied. A set of DNA strands containing the FRET-pair at wisely chosen locations will, thus, make it possible to accurately distinguish distance- from orientation-changes using FRET. In combination with the good nucleobase analog properties this points towards detailed studies of the inherent dynamics of nucleic acid structures. Moreover, the placement of FRET-pair chromophores inside the base stack will be a great advantage in studies where other (biomacro)molecules interact with the nucleic acid. Lastly, our study gives possibly the first truly solid experimental support to the dependence of energy transfer efficiency on orientation of involved transition dipoles as predicted by the Förster theory.

Introduction

In the search for improved methods for more accurate and detailed investigations on the structure and dynamics of nucleic acids as well as their interactions with other (biomacro)molecules we present the first base analog fluorescence resonance energy transfer (FRET)-pair. FRET is a technique frequently utilized to detect structural changes in biomacromolecular systems.[1-5] The strong dependence of the transfer efficiency (E; see eq 1) between an excited donor (D) and a ground state acceptor (A) on distance (R_{DA}^{-6}), makes FRET the obvious choice for monitoring conformational changes and interactions between molecules. The efficiency of energy transfer is also governed by the Förster critical distance, R_0, (eq 2; at which the E is 0.5) which in turn depends on the quantum yield of the donor (ϕ_D), the donor/acceptor spectral overlap integral (J_{DA}), the refractive index of the medium (n), and importantly the geometric factor (κ).[1,2,6]

$$E = R_0^6/(R_0^6+R_{DA}^6) \qquad (1)$$

$$R_0 = 0.211(J_{DA}\kappa^2 n^{-4}\phi_D)^{1/6} \quad \text{in Å} \qquad (2)$$

The geometric factor takes the direction of the donor and acceptor transition dipoles into consideration and is described by eq 3:

$$\kappa = \boldsymbol{e_1}\bullet\boldsymbol{e_2} - 3(\boldsymbol{e_1}\bullet\boldsymbol{e_{12}})(\boldsymbol{e_{12}}\bullet\boldsymbol{e_2}) \qquad (3)$$

where $\boldsymbol{e_1}$ and $\boldsymbol{e_2}$ are the unit vectors of the donor and acceptor transition dipoles and $\boldsymbol{e_{12}}$ the unit vector between their centers. The value of κ^2 can range from 0 to 4. Thus, to be able to extract detailed structural information from the measured FRET efficiency an accurate estimate of κ^2 is required. Such estimates of κ^2 are rarely available due to the lack of knowledge of orientation of the donor or acceptor molecules themselves and/or their interacting transition dipole moments.[7] The most frequently used

(both correctly and incorrectly) κ^2 is 2/3, which corresponds to freely rotating donor and acceptor transition dipoles.

When monitoring conformational changes or interaction processes in nucleic acid containing systems using FRET, the most common method is to covalently attach donor and acceptor molecules *via* flexible linkers to two different positions and to assume that κ^2 is 2/3. However, many donor/acceptor chromophores interact with the nucleic acid structure[7-9] and, thus, the use of a κ^2 of 2/3 is an inaccurate assumption that may result in considerable errors in structural interpretations. Better control of the κ^2 in nucleic acid systems was presented in the excellent study by Lewis *et al.* in which a donor was rigidly attached to one end of the DNA helix resulting in a very good orientation control.[10] However, the acceptor on the opposite end was attached only to one of the strands and had considerable motional freedom. Other recent excellent studies trying to achieve better control of the FRET orientation factor in nucleic acid systems are those by Iqbal *et al.*[11] and Hurley *et al.*[12]. In an attempt to achieve the highest possible control of donor/acceptor orientation we here present a novel FRET-pair composed of two cytosine analogs, tC^O (1,3-diaza-2-oxophenoxazine) and the newly synthesized tC_{nitro} (7-nitro-1,3-diaza-2-oxophenothiazine) (Figure 1).

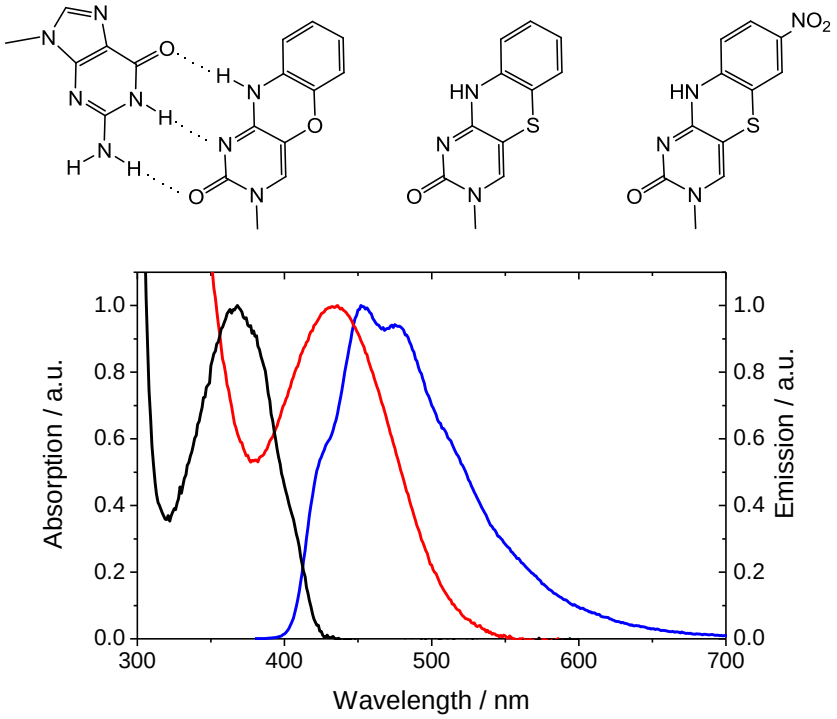

Figure 1. Top: Structure of G-tC^{O} base pair (left), fluorescent cytosine analog tC (middle) and newly developed cytosine analog tC$_{nitro}$ (right). Bottom: Representative normalized absorption (black) and emission (blue) spectra of FRET donor tC^{O} and absorption spectrum (red) of virtually non-fluorescent acceptor tC$_{nitro}$ within dsDNA showing the donor/acceptor spectral overlap. Measurements performed at 22°C in 25 mM phosphate buffer (pH 7.5) and [Na^{+}] = 100 mM.

Results and Discussion

In the design of a nucleic acid base analog FRET-pair, our goal was to utilize tC or tC^{O} (Figure 1). We have previously established that both analogs have a high and stable quantum yield in dsDNA as well as being rigidly stacked within the duplex and, thus, are excellent donor candidates.[13,14-16] With the objective of red-shifting the absorption of tC/tC^{O} and maintaining their nucleobase properties we synthesized tC$_{nitro}$ (Figure 1) as a FRET acceptor.

Before investigating tC$_{nitro}$ as a spectroscopic tool its properties as a cytosine analogue needed to be established. In Table 1 a DNA melting temperature study for duplexes composed of tC$_{nitro}$-containing

strands and the corresponding unmodified complements with G, A, C, and T, respectively, opposite tC_{nitro}/C is presented.

Table 1. DNA Melting Temperatures of tC_{nitro}-containing Duplexes.

	Base opposite tC_{nitro}/C			
DNA sequence [a]	G /ºC [b]	A /ºC [b]	C /ºC [b]	T /ºC [b]
5'-CGTCYTTTGC-3'	47 (45)	32 (21)	28 (20)	32 (27)
5'-CGTTYCTTGC-3'	43 (41)	29 (23)	29 (17)	30 (23)

[a] Y denotes tC_{nitro} or a normal C.

[b] Temperatures in parenthesis are for the unmodified duplexes.

The duplexes where tC_{nitro} is paired with G have melting temperatures that are 13-19ºC higher than when it pairs with A, C, or T on the opposite strand. The corresponding differences for unmodified cytosine are 18-25ºC. Although the differences are slightly lower for the tC_{nitro}/G base-pair than for the normal C/G base-pair, this result shows that tC_{nitro} is highly selective for base-pairing with guanine. In addition, tC_{nitro} increases the melting temperature compared to C by 2ºC in the fully complementary "GC" case. This slight increase in duplex stability is in good agreement with our previous studies on tC and tC^{O}.[13,15] To further establish the suitability of tC_{nitro} as a cytosine analogue when positioned inside the DNA double helix we performed circular dichroism (CD) measurements on the duplexes in Table 1 (see Figure 2). Comparing the modified duplexes (solid lines) to the corresponding unmodified ones (dashed lines) the same overall spectral envelope is found. The general appearance of the CD spectra is that of normal B-form DNA, which is characterized by a positive band centered at 275 nm, a negative band at 250-240 nm, a band that can be either positive or negative at 220 nm, and just below that a narrow negative peak followed by a large positive peak at 190-180 nm.[17] The slight differences that can be seen between the CD of the unmodified and corresponding modified duplex most certainly come as an effect of the differences between the absorption of tC_{nitro} compared to cytosine. In conclusion, the CD experiment together with the duplex melting temperature study, as well as the fact that the structurally very similar tC and tC^{O} have been shown using CD[13,15] and NMR[15] not to alter the natural

form of DNA, indicate that exchanging a cytosine for a tC_{nitro} does not perturb the structure of the normal B-form DNA.

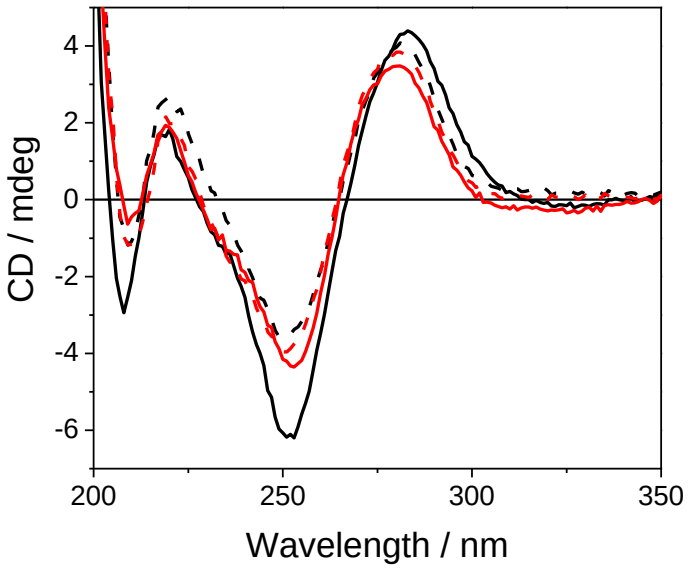

Figure 2. Circular dichroism CD spectra of tC_{nitro}-modified DNA duplexes and the corresponding unmodified duplexes. Modified duplex with CT neighboring tC_{nitro} (black solid line), modified duplex with TC neighboring tC_{nitro} (red solid line) and corresponding unmodified duplexes (dashed lines). Measurements performed in 25 mM phosphate buffer (pH 7.5) and $[Na^+]$ = 100 mM at a duplex concentration of approximately 3.5 µM.

The lowest energy absorption maximum of tC_{nitro} in dsDNA is centered at approximately 440 nm with an extinction coefficient of 5400 $M^{-1}cm^{-1}$ (Figure 1). The position of the absorption results in a very good spectral overlap with the emission of tC^O (Figure 1) which is centered at 465 nm and a smaller overlap with the emission of tC ($Emission_{max}$=505 nm, not shown). In combination with the quantum yield of tC^O in dsDNA and a refractive index of 1.4 in DNA,[1] the R_0 of the tC^O-tC_{nitro} FRET-pair is estimated to be 27 Å when using a κ^2 of 2/3 (the use of 2/3 here is only to facilitate comparison with R_0 of common FRET-pairs). The 33-mer oligonucleotides utilized for the measurements in this study are presented in Table 2.

Table 2. Donor and Acceptor 33-mer Oligonucleotides Used.

Name	Sequence[a]
tC^O1	5'-CGATCACACA**X**AAGGACGAGGATAAGGAGGAGG-3'
tC^O2	5'-CGATCACA**X**ACAAGGACGAGGATAAGGAGGAGG-3'
tC^O3	5'-CGATCA**X**ACACAAGGACGAGGATAAGGAGGAGG-3'
$tC_{nitro}1$	5'-CCTCCTCCTTATCCTCGTC**Y**TTGTGTGTGATCG-3'
$tC_{nitro}2$	5'-CCTCCTCCTTATCCTCGT**Y**CTTGTGTGTGATCG-3'
$tC_{nitro}3$	5'-CCTCCTCCTTATC**Y**TCGTCCTTGTGTGTGATCG-3'
$tC_{nitro}4$	5'-CCTCCTCCTTAT**Y**CTCGTCCTTGTGTGTGATCG-3'

[a] X = tC^O; Y = tC_{nitro}

Except for the FRET donor position, the three tC^O-sequences are the same and are complementary to the tC_{nitro}-sequences, which have the FRET acceptor at four different positions. The positions of the donor and acceptor in the seven sequences are chosen so that every separation between 2 and 13 bases can be monitored combining the strands. Furthermore, the sequences are designed so that tC^O has the same surrounding bases and the donor and acceptor are situated far from the more dynamic ends of the duplex.

Table 3. Lifetimes and Steady-State Quenching Data as well as Fitted FRET Efficiency.

Bases in between	τ_1 (α_1) /ns	τ_2 (α_2) / ns	$\langle\tau\rangle^a$ / ns	χ^2	$1-\langle\tau\rangle/\tau_0$	$1-I/I_0$	E[b]
2	0.05 (0.96)	0.48 (0.04)	0.07	1.24	0.99	0.98	1.00
3	0.05 (0.96)	0.54 (0.04)	0.07	1.31	0.99	0.97	0.99
4	0.13 (0.65)	0.38 (0.35)	0.22	1.14	0.95	0.93	0.98
5	1.11 (0.68)	0.36 (0.32)	0.87	1.62	0.81	0.77	0.89
6	3.64 (1)		3.64	1.28	0.20	0.26	0.18
7	2.63 (1)		2.63	1.57	0.42	0.45	0.39
8	2.65 (1)		2.65	1.58	0.44	0.46	0.55
9	3.09 (1)		3.09	1.30	0.35	0.37	0.43
10	3.91 (1)		3.91	1.14	0.14	0.15	0.17
11	4.41 (1)		4.41	1.11	0.03	0.04	0.01
12	4.40 (1)		4.40	1.13	0.03	0.08	0.02
13	4.26 (1)		4.26	1.21	0.06	0.10	0.05

[a] $\langle\tau\rangle = \alpha_1\tau_{1+}\alpha_2\tau_2$

[b] Fitted FRET efficiency

To study the change in the tC^O-tC_{nitro} FRET efficiency for the 12 different separations, both steady-state and time-resolved fluorescence measurements were performed (Table 3). In both cases the results (Figure 3) show an efficiency that is highly dependent on both distance and orientation as the separation and, thus, the direction of the transition dipoles of the base analogs are altered in a stepwise fashion. The data suggest that we have successfully designed an excellent nucleic acid base analog FRET-pair. In the time-resolved measurements tC^O exhibits single exponential fluorescence decay for most sequences. However, the most quenched sequences need two exponential components in order to explain the fluorescence decay. There might be several reasons for the non-exponential decay such as: (1) difficulties in measuring highly quenched fluorophores on this short timescale where small amounts of unquenched fluorophores or scattered light might disturb the experiment or (2) distribution of donor-acceptor distances and orientations leading to a distribution of energy transfer efficiencies.

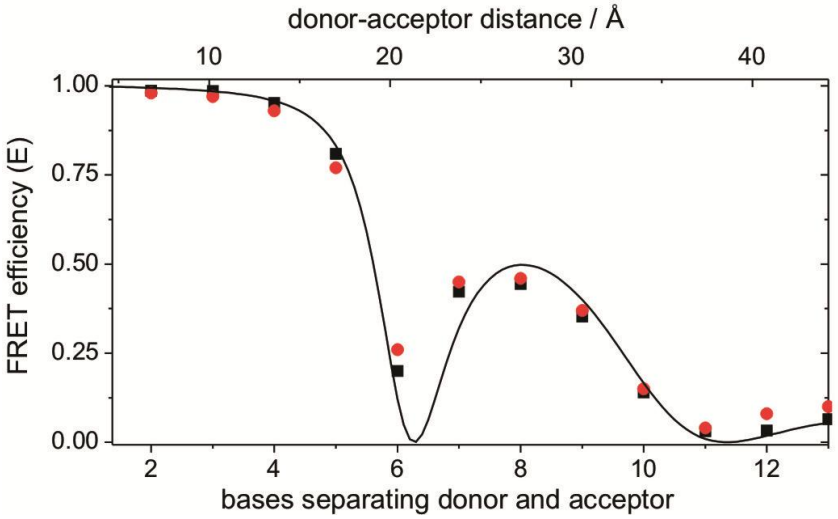

Figure 3. Efficiency of energy transfer for the base analog FRET-pair tC^O-tC_{nitro} estimated using decreases in tC^O, donor, emission (red circles) and tC^O average emission lifetimes (black squares) as the two analogs are separated by 2 to 13 bases in a DNA duplex. Curve fitting using eq 6-7 with α and J_{DA} as fit parameters is shown as solid line. Excitation wavelength 370 nm. Measurements performed at 22°C in 25 mM phosphate buffer (pH 7.5) and $[Na^+]$ = 100 mM.

Qualitatively, the data has an appearance exactly as expected for a FRET-pair situated at different positions within a DNA duplex: *E* decreases sharply with distance while oscillating between local maxima and minima as the transition dipoles of the donor and acceptor change between more parallel and more perpendicular configurations (eq 3). To analyze the measured efficiencies quantitatively we use eq 6 and 7. These equations take into consideration vector distance and accurate orientations between chromophores and become increasingly similar to the rough model in which the chromophores are placed on top of each other along the DNA helix axis, with increasing base separation. The excellent fit, where J_{DA} and α are varied, to the experimental data and the distinct changes between maxima and minima not only confirm that the ϕ_D and the overlap integral (*i.e.* donor emission profile and ε_A) are virtually constant, but also gives further evidence that these C-analogs have practically no dynamics on the time-scale of fluorescence, however, faster dynamics cannot be ruled out. The fit is quite insensitive to the magnitude of the overlap integral and the fitted value ($2 \cdot 10^{14}$ M^{-1} cm^{-1} nm^4) is close to the one estimated from eq. 4 using the spectroscopic properties of the donor and acceptor ($1.2 \cdot 10^{14}$ M^{-1} cm^{-1} nm^4).

From the phase angle parameter in the curve fitting we also find that the direction of the S_1-S_0 transition of tC_{nitro} is rotated 67° compared to that of tC^O within their three-ring systems. This is in good agreement with the values obtained for tC^O (-33°; anti-clockwise from molecule long-axis)[13] and tC_{nitro} (+25°, manuscript in preparation) and proves the high potential of this FRET-pair in detailed structure probing. The slight difference between the curve fitted and the calculated angle of the S_1-S_0-transitions (67° vs. 58°) likely comes as an effect of the model fitting, in combination with small errors in the experimental determination of the transition dipole orientations, rather than any significant changes in orientations when the base analogs are positioned within the base stack compared to their monomeric forms. We have previously performed circular dichroism experiments on homodimers of tC as well as tC^O that are separated by 0-2 bases in DNA-duplexes to examine the excitonic effect and found minor effects for the case where the homodimer is separated only by 0 bases (data not shown). The fact that the exciton interaction found is small most likely comes as an effect of the fairly low extinction

coefficients (oscillator strengths) of the analogs. In the current study we have a case where tC^O and tC_{nitro} are separated by at least 2 bases, the extinction coefficients are fairly low and, furthermore, the energy of the S_1-S_0-transitions of tC^O and tC_{nitro} is different (heterodimer) as is the energy of the S_1-S_0-transitions of tC^O and tC_{nitro} compared to the normal bases. This suggests that the direction of the transition dipoles of tC^O and tC_{nitro} are not substantially affected due to interactions between them or between them and the surrounding bases.

Conclusions

In conclusion we have designed the first nucleic acid base analog FRET-pair. As a consequence of both the analogs being rigidly located within the base stack, this system enables very high control of the orientation factor. A set of strands containing our FRET-pair at strategically chosen positions, *i.e.* where the slopes are steep in Figure 3, will, thus, make it possible to accurately distinguish distance- from orientation-changes using FRET. In combination with the favorable base pairing properties this will facilitate detailed studies of the inherent dynamics of nucleic acid structures. Moreover, the placement of FRET-pair chromophores inside the base stack will be a great advantage in studies where other (biomacro)molecules interact with the nucleic acid. Lastly, our study gives possibly the first truly solid experimental support to the dependence of *E* on orientation of involved transition dipoles as predicted by the Förster theory.

Experimental

Synthesis of nucleoside building blocks tC^O and tC_{nitro}. Unless stated otherwise, all reagents were obtained from commercial suppliers and used without further purification: DCM, pyridine and DIPEA were purified by distillation (over calcium hydride). Synthesis of tC^O, 5-nitro-2-amino-thiophenol and 2-deoxy-3,5-di-*O*-*p*-toluoyl-*α*-D-erythro-pentofuranosyl was done according to literature procedures.[13,18-20] De-oxygenation of reaction mixtures was achieved by bubbling nitrogen through the solution for

30 minutes. Column chromatography was performed using silica gel (Matrex, LC 60Å/35–70 micron). ^{1}H (400 MHz) and ^{13}C (100.6 MHz) NMR spectra were recorded at room temp. in $CDCl_3$ or $(CD_3)_2SO$ using a Jeol Eclipse 400 NMR spectrometer. Chemical shifts are reported relative to residual $CHCl_3$ or $(CH_3)_2SO$ (δ = 7.26 or 2.54 ppm) for ^{1}H NMR and (δ = 77.23 or 40.45 ppm) for ^{13}C NMR, respectively. ^{31}P NMR spectrum was recorded on a Bruker AV300 spectrometer at 121 MHz and was externally referenced to 85% phosphoric acid in deuterated water. High-resolution mass spectrum was recorded using the electrospray technique on a Bruker APEX III FT-ICR mass spectrometer. Low-resolution mass spectra were recorded using the electrospray technique on a Fisons VG platform instrument or a Waters ZMD quadrupole mass spectrometer in acetonitrile (HPLC grade). Elemental analyses were performed by H. Kolbe Mikroanalytisches laboratorium, Mülheim an der Ruhr, Germany.

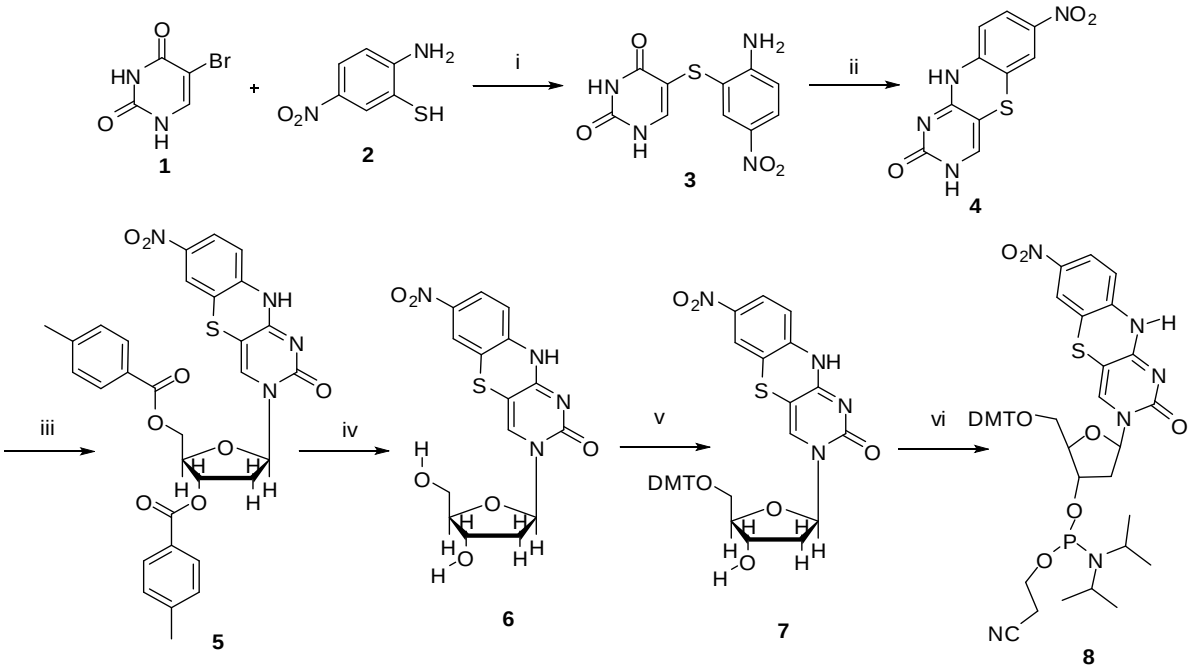

Scheme 1. Reaction conditions: (i) $NaOH_{(aq)}$, 24 h, reflux; (ii) EtOH, HCl, 24 h, reflux, 15% over two steps; (iii) DMF, toluene, 3,5-di-O-*p*-toluoyl-*α*-D-erythro-pentofuranosyl, NaH, 18 h, rt, 11%; (iv) MeONa, MeOH, 18 h, rt, 71%; (v) pyridine, DMAP, DMT-Cl, 18 h, rt, 74%; (vi) DCM, DIPEA, 2-cyanoethyl-N,N-diisopropylchlorophosphoramidite, 1 h, rt, 93%.

3: Degassed NaOH (aq) (0.25 M, 95 ml) was added to a mixture of 5-nitro-2-amino-thiophenol (5.55 g, 32.6 mmol) and 5-bromouracil (6.46 g, 33.8 mmol) under argon and was allowed to reflux for 24 h. The crude product was allowed to cool and was subsequently filtered off. No more purification was done.

4: To the crude product **3** was added EtOH (940 ml) and concentrated HCl (37%, 64 ml). The reaction mixture was refluxed for 24 h where after it was allowed to cool down and subsequently filtered off. The filter cake was slurred up in NH_4 (aq) (8%, 50 ml) at 60°C for 10 minutes, cooled down and filtered off. This was repeated once. The filter cake was washed with water, DMSO and finely MeOH resulting in a red insoluble powder (1.3 g, 5 mmol, 15% over two steps). Elemental analysis calculated for [$C_{10}H_6N_4O_3S$]: C, 45.80; H, 2.31, found C, 45.97; H, 2.36.

5: DMF (15 ml) was added to a mixture of **4** (606 mg, 2.31 mmol) and NaH (60% in mineral oil, 101 mg, 2.54 mmol) under argon. The reaction mixture was left for 1 h where after toluene (15 ml) was added. 2-deoxy-3,5-di-*O*-*p*-toluoyl-*α*-D-erythro-pentofuranosyl (1.04 g, 2.67 mmol) was added portion wise to the blue reaction mixture for 1 h where after it was left overnight. Ethylacetate was added to the mixture where after the mixture was filtrated and the filtrate was washed twice with water where upon the solvent was removed in vacuo. Chromatography (SiO_2, 1-1.5% MeOH in CH_2Cl_2) yielded a yellow-red solid (160 mg, 0.26 mmol, 11%); ^{1}H NMR ($CDCl_3$) δ = 7.88-8.5 (m, 5H), 7.76 (d, 1H), 7.51 (s, 1 H), 7.42 (d, 1H), 7.2-7.3 (m, 4H), 6.32 (dd, 1H), 5.61 (d, 1H), 4.83 (dd, 1H), 4.6-4.7 (m, 2H), 2.94 (dd, 1H), 2.43 (s, 3H), 2.38 (s, 3H), 2.25 (m, 1H) ppm; ^{13}C NMR ($CDCl_3$) δ = 166.2, 160.5, 154.1, 144.7, 144.2, 141.6, 134.7, 130.3, 129.9, 129.7, 129.6, 129.4, 129.2, 126.5, 123.5, 121.4, 118.4, 118.3, 96.1, 87.5, 83.9, 75.1, 64.1, 39.5, 21.8 ppm; Elemental analysis calculated for [$C_{31}H_{26}N_4O_8S$]: C, 60.58; H, 4.26, found C, 60.52; H, 4.31.

6: MeONa (40 mM in MeOH, 25 ml) was added to **5** (137 mg, 0.223 mmol) under argon. The reaction mixture was left overnight where after it was neutralized with acetic acid and the solvent was removed in vacuo. Chromatography (SiO_2, 10-13% MeOH in CH_2Cl_2) yielded a yellow-red solid (60 mg, 0.16 mmol, 71%); ^{1}H NMR ($(CD_3)_2SO$) δ = 11 (br s, 1H), 7.91-8.03 (m, 3H), 7.03 (d, 1H), 6.09 (t, 1H), 5.28

(br s, 1H), 5.15 (br s, 1H), 4.25 (m, 1H), 3.83 (q, 1H), 3.67 (dd, 1H), 3.58 (dd, 1H), 2.21 (m, 1H), 2.07 (m, 1H) ppm; ^{13}C NMR ($(CD_3)_2SO$ δ = 159.66, 154.41, 143.67, 137.30, 124.33, 122.25, 118.70, 117.56, 94.22, 88.53, 86.62, 70.70, 61.71, 41.50 ppm; Elemental analysis calculated for [$C_{15}H_{14}N_4O_6S$]: C, 47.62; H, 3.73, found C, 47.48; H, 3.70.

7: Freshly distilled pyridine (5 ml) was added to **6** (222 mg, 0.587 mmol), DMAP (4 mg, 0.03 mmol) and DMT-Cl (240 mg, 0.71 mmol) under argon. The reaction mixture was left overnight where after it was quenched with a small amount of $NaHCO_3$ (aq, 5%) and the solvent was evaporated in vacuo. The crude product was dissolved in DCM and washed once with 5% $NaHCO_3$ (aq) and twice with H_2O. Chromatography (SiO_2, 1.5-3% MeOH in CH_2Cl_2) yielded a yellow-red solid (297 mg, 0.436 mmol, 74%); ^{1}H NMR ($CDCl_3$) δ = 10.45 (br s, 1H), 7.88 (s, 1H), 7.80 (d, 1H), 7.51 (s, 1H), 7.10-7.45 (m, 10H), 6.83 (m, 4H), 6.37 (t, 1H), 4.68 (m, 1H), 4.17 (m, 2H), 3.74 (s, 3H), 3.71 (s, 3H), 3.41 (d, 1H), 3.33 (d, 1H), 2.88 (m, 1H), 2.34 (m, 1H) ppm; ^{13}C NMR ($CDCl_3$) δ = 160.51, 158.79, 155.20, 144.38, 143.89, 141.82, 136.15, 135.76, 135.39, 130.17, 130.05, 128.21, 128.12, 127.20, 123.21, 121.24, 118.56, 117.78, 113.50, 96.41, 87.43, 87.21, 86.92, 72.10, 63.46, 55.33, 42.32 ppm; Elemental analysis calculated for [$C_{36}H_{32}N_4O_8S$]: C, 63.52; H, 4.74, found C, 63.59; H, 4.67.

8: Dry **7** (0.29 mg, 0.43 mmol) was dissolved in DCM (10.0 mL) under an atmosphere of argon and DIPEA (0.184 mL, 1.06 mmol) was added. 2-cyanoethyl-N,N-diisopropylchlorophosphoramidite (0.114 mL, 0.51 mmol) was then added drop wise and after that the reaction mixture stirred at room temperature for 1 h then transferred under argon into a separating funnel containing degassed DCM (20.0 mL). The mixture was washed with degassed saturated aqueous KCl (20.0 mL) and the organic layer was separated, dried over sodium sulfate, filtered and the solvent removed in vacuo. The phosphoramidite product was dried under vacuum, dissolved in DCM (3 mL) and precipitated from hexane (200 mL) at room temperature to give the title compound **8** (the phosphoramidite of 7-nitro-1,3-diaza-2-oxophenothiazine) as an orange precipitate (0.35 g, 93%); δ_P (300 MHz, $CDCl_3$) 148.21 and 149.14; m/z LRMS [ES$^+$, MeCN] 903 (M + Na^+, 10%); HRMS (M + Na^+) ($C_{45}H_{49}N_6NaO_9PS$) calc. 903.2912, found 903.2895.

Oligonucleotide synthesis. Standard DNA phosphoramidites, solid supports and additional reagents were purchased from Link Technologies or Applied Biosystems Ltd. Disposable Sephadex NAP columns were purchased from GE Healthcare. All oligonucleotides were synthesized on an Applied Biosystems 394 automated DNA/RNA synthesizer using a standard 0.2 μmole phosphoramidite cycle of acid-catalyzed detritylation, coupling, capping, and iodine oxidation. Stepwise coupling efficiencies and overall yields were determined by the automated trityl cation conductivity monitoring facility and in all cases were >98.0%. All β-cyanoethyl phosphoramidite monomers were dissolved in anhydrous acetonitrile to a concentration of 0.1 M. The coupling times were 25 s for normal (A,G,C,T) monomers and 10 min for the modified phosphoramidite monomer. Cleavage of oligonucleotides from the solid support and deprotection was achieved by exposure to concentrated aqueous ammonia solution for 60 min at room temperature followed by heating in a sealed tube for 5 h at 55°C. For details in RP-HPLC analysis and purification of oligonucleotides see Supporting information.

Photophysical measurements

All measurements were made at 22°C in a phosphate buffer at pH 7.5 in total sodium- and phosphate ion concentrations of 100 mM and 25 mM, respectively. Double stranded concentrations were 2 μM or 9 μM (the higher concentration used for time resolved measurements of highly quenched sequences). An excess of the acceptor strand were used in all experiments (to ensure complete hybridization). Absorption spectra were recorded from 200 to 600 nm on a Varian Cary 4000 spectrophotometer. The sequences used in the study are 5'- CGA TCA **X**A**X** A**X**A A**YY** ACG A**YY** ATA AGG AGG AGG -3', where X is C which can be substituted by a tC^O and Y is a G where the C on the complementary strand can be substituted by a tC_{nitro}. Combination of singly substituted strands results in duplexes with distances ranging from 2 to 13 base pairs separating the tC^O and tC_{nitro} (10 Å to 48 Å). The extinction coefficient of the tC_{nitro} nucleoside was determined by measuring the absorption of samples of known concentration. Samples were prepared by weighing out small amounts of the tC_{nitro} nucleoside, typically

1 mg, and dissolving them in known volumes of MQ water (Millipore). The extinction coefficient was determined as an average of three measurements.

Steady state fluorescence was measured on a Spex Fluorolog 3 spectrofluorimeter (JY Horiba). The emission spectra were recorded from 380 to 800 nm with the excitation wavelength fixed at 370 nm.

Fluorescence lifetimes were determined using time-correlated single photon counting. The excitation pulse was provided by a Tsunami Ti:Sapphire laser (Spectra-Physics; 80 MHz) which was pumped by a Millenia Pro X (Spectra-Physics). The Tsunami output at 740 nm was acousto-optically pulse-picked to 4 MHz by a pulse selector (Spectra Physics) when needed and subsequently frequency-doubled yielding an excitation wavelength of 370 nm. The photons were collected by a thermoelectrically cooled micro channel-plate photomultiplier tube (MCP-PMT R3809U-50; Hamamatsu) and fed into a multi-channel analyzer with 4096 channels. A minimum of 10000 counts were recorded in the top channel. The fluorescence decay curves were fitted to exponential expressions by the program FluoFit Pro v.4 (PicoQuant GmbH). The sample response was monitored through a monochromator at 460±16 nm.

UV absorption DNA melting studies were performed on 10-mer oligonucleotides (for sequences see Table 1 or Supporting Information) at a concentration of approximately 4 μM using a Varian Cary 4000 spectrophotometer equipped with a programmable multi-cell temperature block. The samples were heated from 10°C to 80°C at a maximum rate of 0.2°C min^{-1} whereupon they were cooled to 10°C at the same rate. The absorption at 260 nm was measured with a temperature interval of 0.5°C. Melting temperatures were determined using the maximum of the derivatives.

Circular Dichroism spectra were recorded on 10-mer oligonucleotides (for sequences see Table 1 or Supporting Information) at a concentration of approximately 3.5 μM using a Jasco J-810 spectropolarimeter at 20ºC. Spectra were recorded between 200 and 500 nm.

Theoretical evaluation

The energy transfer efficiency for the steady state case as well as for the time resolved case was determined using eq 4:

$$E = 1 - \frac{F}{F_0} = 1 - \frac{\langle \tau \rangle}{\tau_0} \qquad (4)$$

where E is the energy transfer efficiency, F and F_0 are the integrated emission intensities of the donor in presence and absence of acceptor, respectively, and τ and τ_0 are the donor lifetimes in presence and absence of acceptor, respectively. The expected energy transfer efficiencies were calculated using eq 1 and the Förster distances, R_0, were calculated using eq 2 with the refractive index (n) and donor quantum yield (ϕ_D) set to 1.4 and 0.23, respectively.[1,13] The spectral overlap integral (J_{DA}) was determined using eq 5:

$$J_{DA} = \int_0^\infty F_D(\lambda)\varepsilon_A(\lambda)\lambda^4 d\lambda \qquad (5)$$

where F_D is the normalized donor emission and ε_A is the acceptor absorption. The orientation factor, κ, was calculated using eq 6:[21]

$$\kappa_{DA} = \cos(n_{DA}\beta + \alpha) - 3\left(\frac{a \bullet \sin(n_{DA}\beta + \alpha)}{R_{DA}}\right)^2 \qquad (6)$$

where n_{DA} is the number of base pairs in between the donor and acceptor, a is the distance between the centre of the DNA helix to the centre of the chromophore (4 Å), R_{DA} is the donor acceptor distance, α is a fitted phase angle, and β is the helical rise angle (34.3° /base pair). The donor acceptor distance (in Å) is calculated using eq 7:[21]

$$R_{DA} = \sqrt{2a^2(1 - \cos(n_{DA}\beta + \alpha)) + (b(n_{DA} + 1))^2} \qquad (7)$$

where b is the helical rise (3.4 Å /base pair). An in-house made MATLAB program was used to fit the data from the lifetime measurements with respect to the phase angle and the overlap integral. The phase angle is defined as the angle between the transition dipole moments of the donor on one strand and the acceptor on the other, looking along the DNA helix long-axis and when there are no bases separating the donor and the acceptor (*i.e.* the acceptor is the neighboring base of the guanine that base-pairs with the donor). Considering how the donor and acceptor are oriented in the helix, the phase angle can be

translated to an angle describing the difference in the orientation of the transition dipole moments of the donor and acceptor within their three-ring systems.

Acknowledgment. Prof. Kristine Kilså at the University of Copenhagen is acknowledged for fruitful discussions. This research is supported by the Swedish Research Council.

Supporting Information Available. Details in RP-HPLC analysis and purification of oligonucleotides. This material is available free of charge via the Internet at http://pubs.acs.org.

References

(1) Lakowicz, J. R. *Principles of Fluorescence Spectroscopy*; 2nd ed.; Springer: New York, 2006.
(2) Clegg, R. M. *Methods in Enzymology* **1992**, *211*, 353-388.

(3) Clegg, R. M.; Murchie, A. I. H.; Zechel, A.; Lilley, D. M. J. *Proc. Natl. Acad. Sci. U.S.A.* **1993**, *90*, 2994-2998.
(4) Murchie, A. I. H.; Clegg, R. M.; von Kitzing, E.; Duckett, D. R.; Diekmann, S.; Lilley, D. M. J. *Nature* **1989**, *341*, 763-766.
(5) Stengel, G.; Gill, J. P.; Sandin, P.; Wilhelmsson, L. M.; Albinsson, B.; Nordén, B.; Millar, D. P. *Biochemistry* **2007**, *46*, 12289-12297.
(6) Dale, R. E.; Eisinger, J. *Biopolymers* **1974**, *13*, 1573-1605.
(7) Dolghih, E.; Roitberg, A. E.; Krause, J. L. *J. Photochem. Photobiol., A* **2007**, *190*, 321-327.
(8) Norman, D. G.; Grainger, R. J.; Uhrin, D.; Lilley, D. M. J. *Biochemistry* **2000**, *39*, 6317-6324.
(9) Iqbal, A.; Wang, L.; Thompson, K. C.; Lilley, D. M. J.; Norman, D. G. *Biochemistry* **2008**, *47*, 7857-7862.
(10) Lewis, F. D.; Zhang, L. G.; Zuo, X. B. *J. Am. Chem. Soc.* **2005**, *127*, 10002-10003.
(11) Iqbal, A.; Arslan, S.; Okumus, B.; Wilson, T. J.; Giraud, G.; Norman, D. G.; Ha, T.; Lilley, D. M. J. *Proc. Natl. Acad. Sci. U.S.A.* **2008**, *105*, 11176-11181.
(12) Hurley, D. J.; Tor, Y. *J. Am. Chem. Soc.* **2002**, *124*, 13231-13241.
(13) Sandin, P.; Börjesson, K.; Li, H.; Mårtensson, J.; Brown, T.; Wilhelmsson, L. M.; Albinsson, B. *Nucleic Acids Res.* **2008**, *36*, 157-167.
(14) Wilhelmsson, L. M.; Holmén, A.; Lincoln, P.; Nielsen, P. E.; Nordén, B. *J. Am. Chem. Soc.* **2001**, *123*, 2434-2435.
(15) Engman, K. C.; Sandin, P.; Osborne, S.; Brown, T.; Billeter, M.; Lincoln, P.; Nordén, B.; Albinsson, B.; Wilhelmsson, L. M. *Nucleic Acids Res.* **2004**, *32*, 5087-5095.
(16) Sandin, P.; Wilhelmsson, L. M.; Lincoln, P.; Powers, V. E. C.; Brown, T.; Albinsson, B. *Nucleic Acids Res.* **2005**, *33*, 5019-5025.
(17) Rodger, A. and Nordén, B. (1997) *Circular Dichroism and Linear Dichroism.* Oxford University Press, Oxford, NY.
(18) Lin, K. Y.; Jones, R. J.; Matteucci, M. *J. Am. Chem. Soc.* **1995**, *117*, 3873-3874.
(19) Rolland, V.; Kotera, M.; Lhomme, J. *Synthetic Commun.* **1997**, *27*, 3505-3511.
(20) Chedekel, M. R.; Sharp, D. E.; Jeffery, G. A. *Synthetic Commun.* **1980**, *10*, 167-173.
(21) Carlsson, C.; Larsson, A.; Björkman, M.; Jonsson, M.; Albinsson, B. *Biopolymers* **1997**, *41*, 481-494.

TOC Graphic

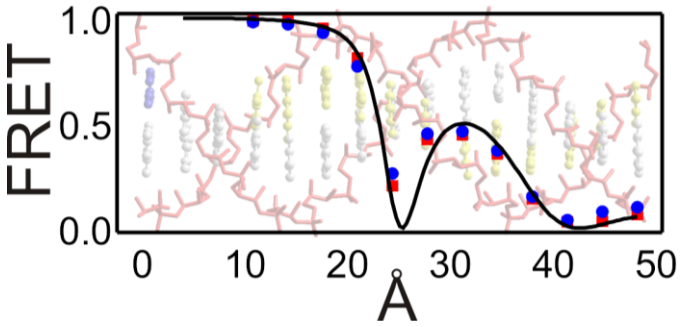
FRET
1.0
0.5
0.0
0
10
20
30
40
50
Å